Available online at www.sciencedirect.com
ScienceDirect
Dyes and Pigments 74 (2007) 237–248
DYES and PIGMENTS
www.elsevier.com/locate/dyepig

Recycling coir pith, an agricultural solid waste, for the removal of procion orange from wastewater

D. Kavitha*, C. Namasivayam

Environmental Chemistry Division, Department of Environmental Sciences, Bharathiar University, Coimbatore-641 046, India

Received 16 October 2005; received in revised form 17 December 2005; accepted 31 January 2006
Available online 2 May 2006

Abstract

Batch adsorption experiments were carried out for the removal of procion orange from its aqueous solution using coir pith carbon. This study examines adsorption kinetic parameters on coir pith carbon. The effect of process parameters like contact time, concentration of dye, temperature and pH on the extent of procion orange adsorption from solution has been investigated. In order to develop an effective and accurate design model for removal of dye, adsorption kinetics and equilibrium data are essential basic requirements. Kinetic study showed that the adsorption of dye on coir pith carbon was a gradual process. Lagergren first-order, second-order, Bangham's and intra-particle diffusion model were used to fit the experimental data. Results of the kinetic studies show that the adsorption reaction is second-order kinetic model with respect to dye solution concentration. Equilibrium isotherms were analyzed by Langmuir, Freundlich, Dubnin–Radushkevich, and Tempkin isotherms. The adsorption equilibrium data obeyed Langmuir, Dubnin–Radushkevich, and Tempkin isotherms. The adsorption capacity was found to be 2.6 mg/g of carbon. Increase of temperature increased adsorption. Acidic pH was favorable for the adsorption of dye. Studies on pH effect and desorption show that chemisorption seems to play a major role in the adsorption process.

Keywords: Adsorption; Procion orange; Coir pith carbon; Isotherms; Kinetics; Temperature study

1. Introduction

Removal of color from wastewater is a most challenging and perplexing problem. The colored wastewaters from these industries are harmful to the aquatic life in rivers and lakes due to reduced light penetration and the presence of highly toxic metal complex dyes. Dyes can cause allergic dermatitis, skin irritation, cancer, mutation, etc. Most of the industries like textile, leather, plastics, paper, food, cosmetics, etc., use dyes and pigments to color their products. Although the exact number and amount of dyes produced in the world is not known, it is estimated to be more than 100,000 with over 7×10^5 tons of dye-stuff produced annually [1–3].

A large number of reactive dyes are azo compounds that are linked by an azo bridge [4]. Even the presence of very low concentrations of dyes (less than 1 mg/L) in the effluent is highly visible and is considered undesirable [5]. In addition, since reactive dyes are highly soluble in water, their removal from effluent is difficult by conventional physicochemical and biological treatment methods [6,7].

Photocatalytic degradation of reactive dye using sunlight/ZNO [8], by ozonation [9] and in a bubble-column reactor [10], electrochemical process by manganese mineral [11], coagulation [12], ozone membrane separation [13], anaerobic decolourisation [14], advanced oxidation with UV/H_2O_2 and adsorption on GAC [15], granulated iron hydroxide and its oxidative regeneration for adsorption of reactive dyes have also been investigated [16].

Wastewaters from dyeing industries are released into nearby land or rivers without any treatment because the conventional treatment methods are not cost effective in the Indian context. On the other hand, low-cost technologies do

* Corresponding author. Hallym University, Department of Environmental Sciences and Biotechnology, 1 Okchon-dong, Chuncheon, Gangwon-do 200-702, Republic of Korea. Tel.: +82 33 248 2165; fax: +82 33 241 1536.
E-mail address: srikavi1@gmail.com (D. Kavitha).

0143-7208/$ - see front matter © 2006 Elsevier Ltd. All rights reserved.
doi:10.1016/j.dyepig.2006.01.040

not allow a wishful color removal or have certain disadvantages. Adsorption is one of the most effective methods and activated carbon is the preferred adsorbent widely employed to treat wastewater containing different classes of dyes.

In these respects, adsorption has been found to be an efficient and economically cheap process for removing dyes using various adsorbents [17,18]. For removal of color from industrial wastewater, adsorption has become one of the most economic and effective method. Thus this process has aroused considerable interest during recent years. The adsorption of impurities from solution onto solid materials currently offers an attractive method of wastewater treatment.

Adsorption is a surface phenomenon, involving the accumulation of dissolved or suspended contaminants on surfaces of activated carbon within an equilibrium phenomenon. The process is superior to many other methods of water reuse by virtue of its low initial cost, low energy requirements, simplicity of design, and possibility of reusing the spent carbon via regeneration [19].

A number of investigators have studied the feasibility of using inexpensive alternative materials like rice husk [20], barley husk [21], coconut based powdered activated carbon [5], de-oiled soya [22], spent brewery grains [23], bagasse fly ash [24], chitson [25], peanut hull [26], neam leaf powder [27] etc., as carbonaceous precursors for the removal of dyes from wastewater.

For any batch adsorption process, the main parameters to be considered are pH, temperature, particle size and time [28]. Hence it is necessary to investigate extensively on the relationship between adsorption efficiency and the parameters affecting it. Owing to high cost of activated carbon, an adsorbent that is cheap and easily available would be a better alternative. In the present study, a novel adsorbent consisting of coir pith carbon was investigated for its efficiency in the removal of dye, namely procion orange, from aqueous solution. Their molecular structure is shown in Fig. 1. The interaction between the parameters was studied.

2. Experimental

2.1. Physicochemical analysis of adsorbent

Coir pith was collected from nearby coconut coir industries, dried in sunlight for 5 h and ground. The dried coir pith powder was sieved to 250–500 μm size. It was subjected to carbonization at 700 °C for 1 h using a muffle furnace under closed conditions. The carbonized material was taken out, sieved to 250–500 μm size again and used for adsorption studies. Morphological features of samples were obtained with a Hitachi 2300 Scanning Electron Microscope. The characteristics of the coir pith carbon have been reported in Table 1.

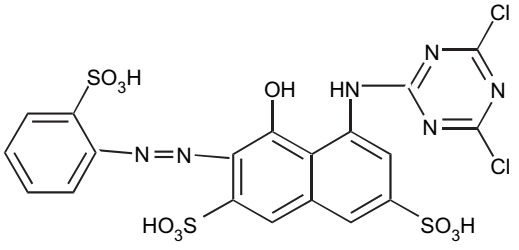

Fig. 1. Molecular structure of procion orange (Acid Blue 15) C.I. No. 42645.

2.2. Experimental procedure

Adsorption experiments were carried out by agitating 300 mg of carbon with 50 ml of dye solution of desired concentration and pH at 200 rpm, 35 °C, in a thermostated rotary shaker (ORBITEK, Chennai, India). Procion orange concentration was estimated spectrophotometrically by monitoring the absorbance at 492.6 nm using UV–vis spectrophotometer (Hitachi, model U-3210, Tokyo). pH was measured using pH meter (Elico, model LI-107, Hyderabad, India). The dye solution was separated from the adsorbent by centrifugation at 20,000 rpm for 20 min and its absorbance was measured. Effect of adsorbent dosage was studied with different adsorbent doses (25–400 mg) and 50 ml of dye solutions and agitated for equilibrium time. Langmuir, Freundlich, Dubinin and Radushkevich and Tempkin equations were employed to study the equilibrium adsorption. Effect of pH was studied by adjusting the pH of dye solutions using dilute HCl and NaOH solutions and the solutions were agitated with 200 mg/50 ml adsorbent dose at 40 and 60 min, respectively, for 10 and 20 mg/L dye concentrations. The adsorbent that was used for the adsorption of 10 or 20 mg/L of dye solution was separated from the solution by centrifugation and desorption studies were conducted. The dye-loaded adsorbent was filtered using Whatman filter paper and washed gently with water to remove any unadsorbed dye. Several such samples were prepared. Then the spent adsorbent was agitated for 25, and 70 min with 50 ml of distilled water, adjusted to different pH values. The desorbed dye was estimated as before. For temperature studies, adsorption of 10 mg/L of procion orange by 200 mg of adsorbent was carried out at 35, 40, 50 and 60 °C in the thermostated rotary shaker.

Table 1
Characteristics of coir pith carbon

Physical parameters			
Specific surface area (m^2/g)	167	pH_{ZPC}	8.0
Bulk density (g/mL)	0.12	pH (1% solution)	10.1
Conductivity (1% solution) (mS/cm)	2.3	Ash content (%)	79.87
Mechanical moisture content (%)	5.88	Porosity (%)	93.11
Specific gravity	1.742	Volatile matter (%)	58.38
Decolourising power (mg/g)	21.0	Fixed carbon (%)	41.62
Iodine number (mg/g)	101.52	Ion exchange capacity	Nil
Chemical parameters			
Sodium (%)	0.14	Potassium (%)	0.18
Calcium (%)	0.22	Phosphorous (%)	0.01
Iron (%)	0.18		

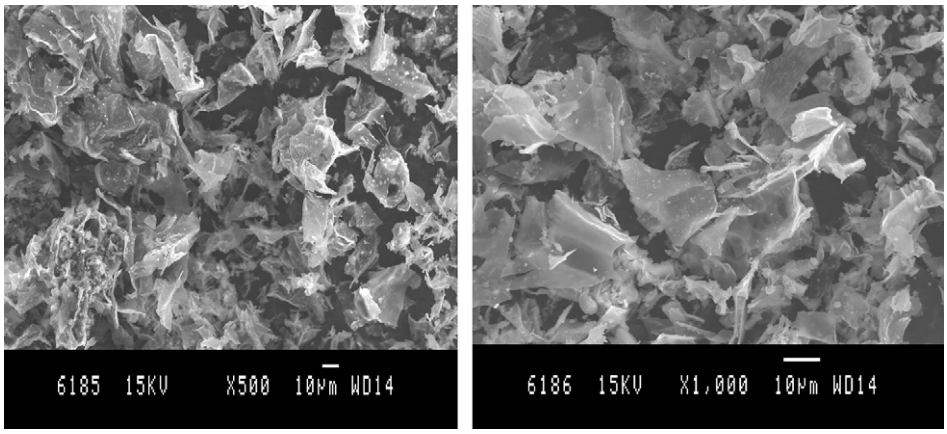

Fig. 2. Scanning electron micrograph of coir pith carbon.

3. Results and discussion

3.1. Scanning electron micrograph studies

SEM is widely used to study the morphological features and surface characteristics of the adsorbent materials [29,30]. In the present study, scanning electron microscopic photograph (Fig. 2) of coir pit carbon reveals surface texture and porosity. This photomicrograph shows fibrous structure of coir pith carbon.

Table 2
Kinetic parameters for the removal of procion orange by coir pith carbon

Pseudo-first-order constants							
Conc	k_1 (min^{-1})	q_e (mg/g)	R^2	Temp (°C)	k_1 (min^{-1})	q_e (mg/g)	R^2
10	0.083	0.399	0.978	35	0.029	0.540	0.981
20	0.156	0.626	0.952	40	0.033	0.462	0.965
30	0.709	0.486	0.985	50	0.032	0.347	0.972
40	0.713	0.592	0.970	60	0.029	0.275	0.950

Pseudo-second-order constants							
Conc	h (mg/g min)	k_2 (g/mg min)	R^2	Temp (°C)	h (mg/g min)	k_2 (g/mg min)	R^2
10	1.244	0.713	0.999	35	0.399	0.215	0.997
20	2.231	0.544	0.999	40	0.542	0.274	0.998
30	3.069	0.629	0.999	50	0.811	0.396	0.999
40	3.114	0.518	0.999	60	1.132	0.531	0.999

Bangham constants							
Conc	k_0 (ml/g/L)	α	R^2	Temp (°C)	k_0 (ml/g/L)	α	R^2
10	15.957	0.1147	0.9915	35	26.353	0.1002	0.9959
20	8.276	0.1017	0.9901	40	19.228	0.1601	0.9683
30	5.799	0.0765	0.9939	50	22.984	0.1261	0.9909
40	4.429	0.0874	0.9808	60	16.249	0.1859	0.9846

Intra-particle diffusion constants					
Conc	k_{id} (mg/g min)	R^2	Temp (°C)	k_{id} (mg/g min)	R^2
10	0.0852	0.9858	35	0.0681	0.9715
20	0.1201	0.9728	40	0.0596	0.9451
30	0.1038	0.993	50	0.0473	0.9288
40	0.1288	0.9633	60	0.0377	0.9006

3.2. Effects of agitation time and concentration of dye on adsorption

The nature of adsorption process will depend on physical or chemical characteristics of the adsorbent and also on the system conditions. The amount of dye adsorbed (mg/g) increased with increase in agitation time and reached equilibrium. The equilibrium time was 30 min for all dye concentrations. The amount of dye removal at equilibrium increased from 1.34 to 2.44 mg/g with the increase in dye concentration from 10 to 40 mg/L. It is clear that the removal of dyes depends on the concentration of the dye. It is also observed that for an initial dye concentration of 10 mg/L, maximum amount (approximately 80.5% of total amount of dye removed) of dye was adsorbed within the first 30 min at an average adsorption rate of 0.0448 mg/g min, and thereafter the adsorption rate tends to decrease and proceeds at an average adsorption rate of 0.0159 mg/g min. A similar trend was observed for the remaining range of initial dye concentrations (20–40 mg/L) studied. The initial rapid phase may be due to the increased number of vacant sites available at the initial stage, as a result there exist increased concentration gradient between adsorbate in solution and adsorbate in the adsorbent.

3.3. Adsorption dynamics

The rate constant of adsorption is determined from the first-order rate expression given by Lagergren [31]

$$\log(q_e - q) = \log q_e - k_l t/2.303 \quad (1)$$

where q_e and q are the amounts of dye adsorbed (mg/g) at equilibrium and at time t (min), respectively, and k_1 is the rate constant of adsorption (l/min). Values of k_1 were calculated from the plots of log (q_e–q) versus t (Figure not shown) suggesting the first-order kinetics of the removal of procion orange. The values of k_1 and q_e at different concentrations calculated from the slops and intercepts of these curves are represented in Table 2.

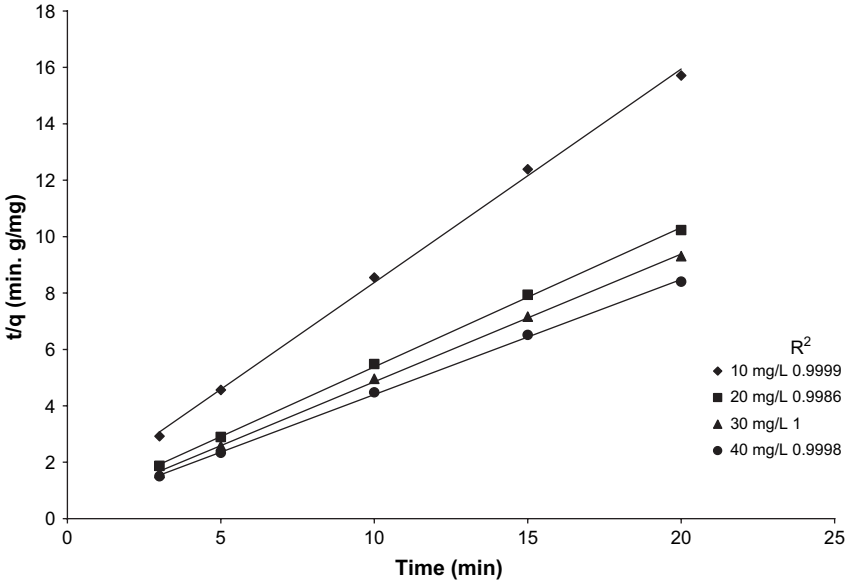

Fig. 3. Second-order kinetic plots for the removal of procion orange: at different initial dye concentrations: adsorbent dose, 300 mg/50 ml; initial pH, 6.9; temperature, 35 °C.

3.4. The second-order kinetic model

The second-order kinetic model [32] is expressed as

$$t/q = 1/k_2 q_e^2 + t/q_e \quad (2)$$

The initial adsorption rate, h (mg/g min), as $t \to 0$ can be defined as

$$h = k_2 q_e^2 \quad (3)$$

The initial adsorption rate (h), the equilibrium adsorption capacity (q_e), and the second-order constants k_2 (g/mg min) can be determined experimentally from the slope and intercept of plot t/q versus t (Fig. 3). Calculated correlations are closer to unity for second-order kinetics model; therefore the adsorption kinetics could well be approximated more favourably by second-order kinetic model for procion orange. The k_2 (g/mg min) and h (mg/g min) values as calculated from Fig. 3 are listed in Table 2. Similar phenomena have been observed in the adsorption of congo red and 2-chlorophenol on coir pith carbon [5,7].

3.5. Intra-particle diffusion study

An empirically found functional relationship, common to most adsorption processes, is that the uptake varies almost

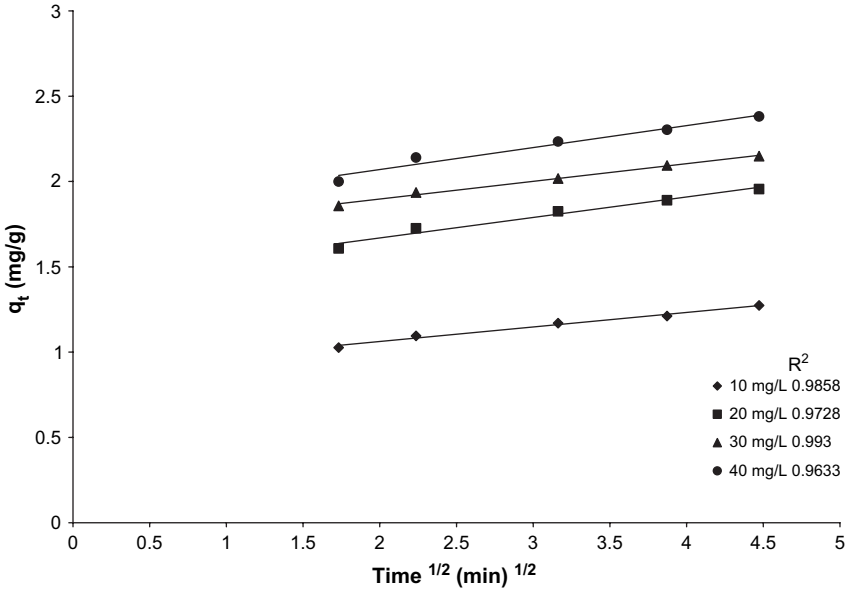

Fig. 4. Weber and Morris intra-particle diffusion plots for removal of procion orange at different initial dye concentrations: adsorbent dose, 300 mg/50 ml; initial pH, 6.9; temperature, 35 °C.

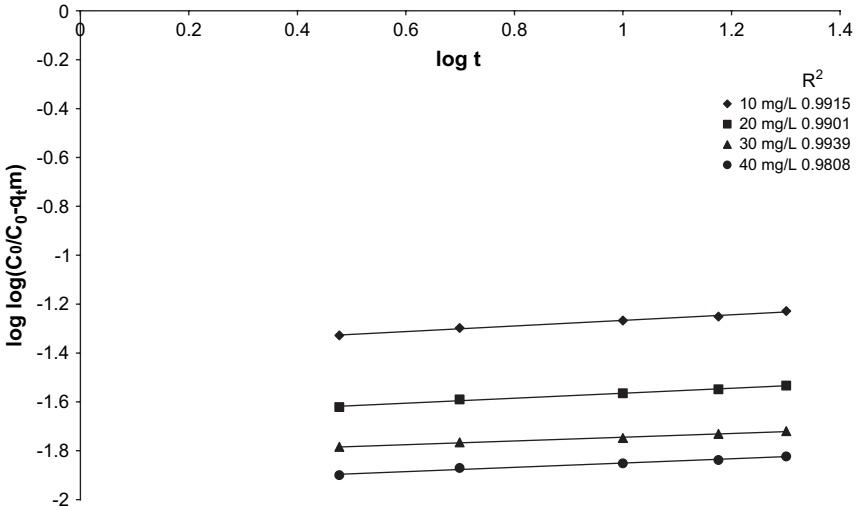

Fig. 5. Bangham's plot for removal of procion orange at different initial dye concentrations: adsorbent dose, 300 mg/50 ml; initial pH, 6.9; temperature, 35 °C.

proportionally with $t^{1/2}$, the Weber–Morris plot, rather than with the contact time, t [33]

$$q_t = k_{id} t^{1/2} + C \quad (4)$$

where k_{id} is the intra-particular diffusion rate constant. According to Eq. (4), a plot of q_t versus $t^{1/2}$ should be a straight line with a slope k_{id} and intercept C when adsorption mechanism follows the intra-particular diffusion process. Values of the intercept give an idea about the thickness of boundary layer, i.e., the larger the intercept the greater is the boundary layer effect [34]. In Fig. 4, plot of mass of dye adsorbed per unit mass of adsorbent, q_t versus $t^{1/2}$, is presented for procion orange. The linear plots are attributed to the macropore diffusion, which is the accessible sites of adsorption. This is attributed to the instantaneous utilization of the most readily available adsorbing sites on the adsorbent surface. The values of k_{id} as obtained from the slope of straight lines are listed in Table 2.

3.6. Bangham's equation

Kinetic data were further used to know about the slow step occurring in the present adsorption system using Bangham's equation [35]

$$\log\log(C_0/C_0 - q_t m) = \log(k_0 m/2.303V) + \log(t) \quad (5)$$

where C_0 is the initial concentration of adsorbate in solution (mg/L), V is the volume of solution (ml), m is the weight of adsorbent per liter of solution (g/L), q_t (mg/g) is the amount of adsorbate retained at time t, and α (<1) and k_0 are constants. The double logarithmic plot (Fig. 5) according to the above equation yielded perfect linear curves for procion orange removal by carbon showing that the diffusion of adsorbate into pores of the adsorbent is not the only rate controlling step [36].

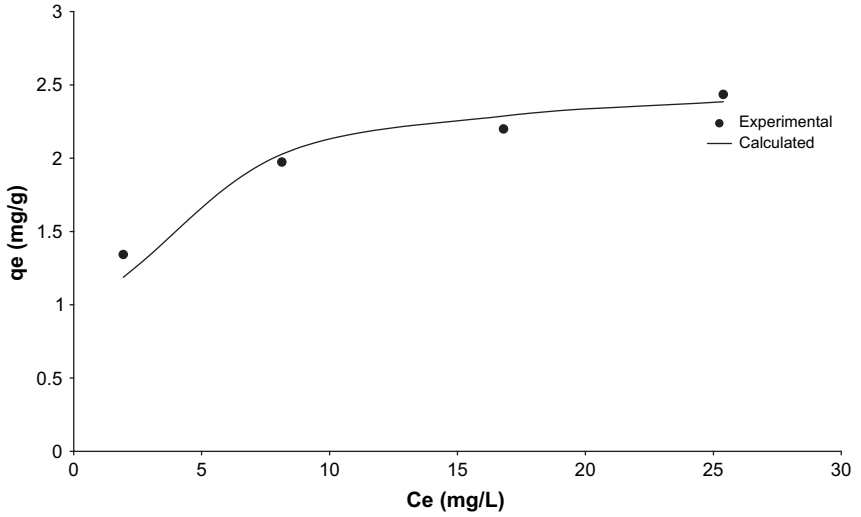

Fig. 6. Langmuir plot for the adsorption of procion orange by coir pith carbon.

Table 3
Isotherm parameters for removal of procion orange by coir pith

Langmuir constants			
Conc	Q_0 (mg/g)	b (L/mg)	R_L
10	2.60	0.433	0.188
20			0.104
30			0.072
40			0.055
Freundlich constants			
Conc	k_f ($mg^{1-(1/n)} L^{1/n} g^{-1}$)	n	R^2
10	0.875	2.367	0.8235
20	0.332	1.260	0.7932
30	0.073	0.819	0.7429
40	0.019	0.661	0.7154
Dubnin–Radushkevich constants			
Conc	q_s (mg/g)	E (kJ/mol)	R^2
10	6.41	1.0	0.9256
20			
30			
40			
Tempkin constants			
Conc	K_t (1/mg)	B_1	R^2
10	13.39	0.4143	0.9947
20			
30			
40			

3.7. Adsorption equilibrium study

To optimize the design of an adsorption system for the adsorption of procion orange, it is important to establish the most appropriate correlation for the equilibrium curves. Various isotherm equations have been used to describe the equilibrium nature of adsorption. Some of these equations are Langmuir, Freundlich, Dubinin and Radushkevich and Tempkin equations.

3.7.1. Adsorption isotherms

Langmuir isotherm [37] is represented by the following equation:

$$C_e/q_e = 1/Q_0 b + C_e/Q_0 \quad (6)$$

where C_e is the concentration of dye solution (mg/L) at equilibrium. The constant Q_0 signifies the adsorption capacity (mg/g) and b is related to the energy of adsorption (L/mg). Values of Q_0 and b calculated in the removal of procion orange using orange peel [38] adsorbent are 1.33 and 0.059, respectively.

Langmuir plot is shown in Fig. 6 along with the experimental data. Langmuir plot is a better fit of the experimental data compared to Freundlich plots. Values of Q_0 and b were calculated from the slope and intercept of the linear plots and are presented in Table 3.

The essential characteristics of the Langmuir isotherm can be expressed by a dimensionless constant called equilibrium parameter R_L, defined by Weber and Chakkravorti [39]:

$$R_L = 1/(1 + bC_0) \quad (7)$$

where b is the Langmuir constant, C_0 is the initial dye concentration (mg/L), and R_L values indicate the type of isotherm. The calculated R_L values versus initial solute concentration were represented in Fig. 7 and Table 3 shows R_L values between zero and one, which confirms the favorable uptake of procion orange.

3.7.2. Freundlich isotherm

Freundlich isotherm [40] was also applied to plot the equilibrium data of the adsorption

$$\log_{10}(x/m) = \log_{10} k_f + (1/n)\log_{10} C_e \quad (8)$$

where x is the amount of dye adsorbed (mg), m is the weight of the adsorbent used (g), C_e is the equilibrium concentration of dye in solution (mg/L), and k_f ($mg^{1-(1/n)} L^{1/n} g^{-1}$) and $1/n$ are

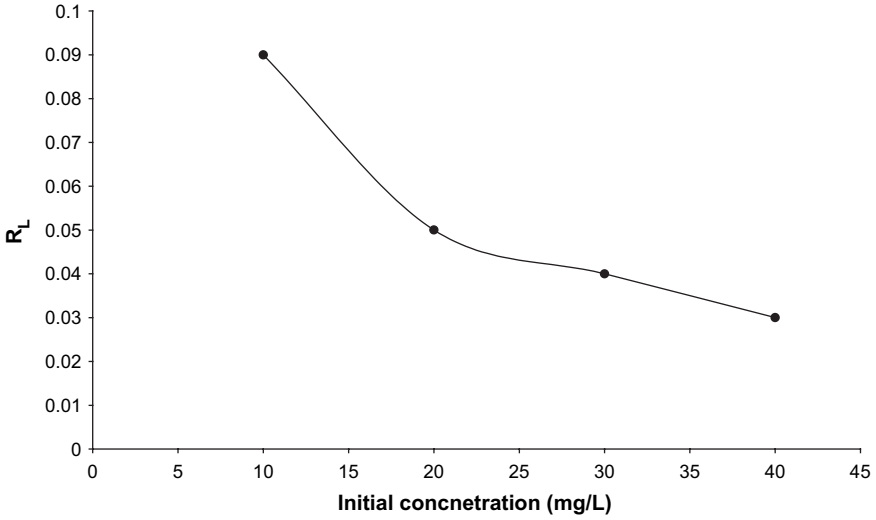

Fig. 7. Separation factor for procion orange onto coir pith carbon.

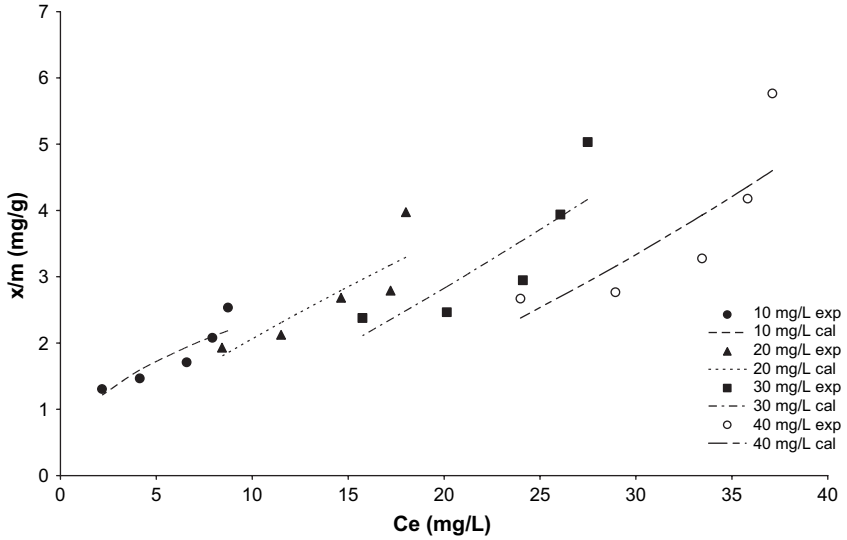

Fig. 8. Freundlich plots for the adsorption of procion orange by coir pith carbon.

Freundlich constants. n is related to the adsorption energy distribution and k_f indicates the adsorption capacity. Freundlich plots are shown in Fig. 8 along with the experimental data. Freundlich plots do not fit satisfactorily with the experimental data. The correlation coefficients were found to be less than 0.8 (Fig. 8) and values of k_f and n were calculated from the intercept and slope of the plots and are presented in Table 3. Calculated values of k_f and n in the removal of procion orange peel [38] as adsorbent are 0.164 and 2.072 respectively.

3.7.3. Dubinin and Radushkevich isotherm

This isotherm is generally expressed as follows [41]:

$$q_e = q_s \exp\left(-B\,\varepsilon^2\right) \tag{9}$$

where q_s is D–R constant and ε can be correlated:

$$\varepsilon = \mathrm{RT}\ln(1 + 1/C_e) \tag{10}$$

The constant B gives the mean free energy E of adsorption per molecule of adsorbate when it is transferred to the surface of the solid from infinity in the solution and can be computed using the following relationship [42]:

$$E = 1/(2B)^{1/2} \tag{11}$$

Calculated Dubinin–Radushkevich constants for the adsorption of procion orange on coir pith carbon are shown in Table 3; the D–R isotherms are plotted against the experimental data points, as shown in Fig. 9. From this figure, it is clear that the adsorption energy value is lowest for adsorption of procion orange on coir pith carbon. The values of correlation coefficients are much lower than the other three isotherm values. In this case, the D–R equation represents the poorer fit of experimental data than the other isotherm equation.

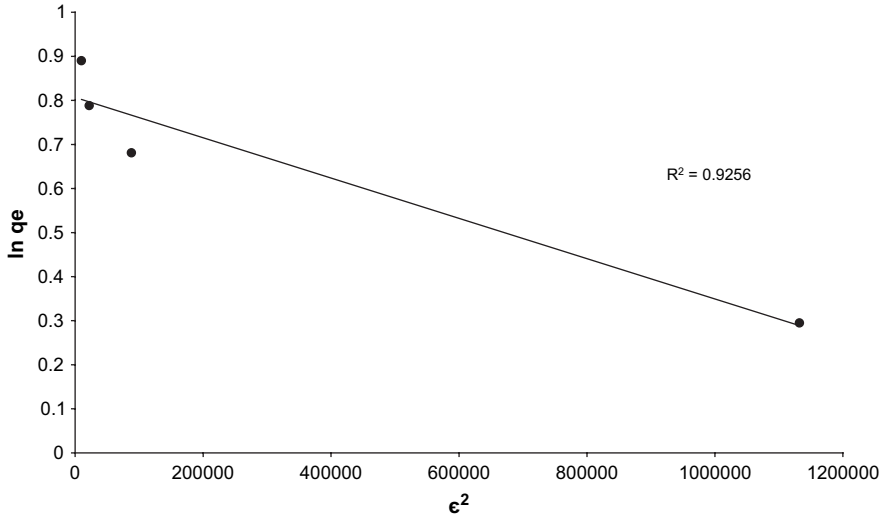

Fig. 9. Dubnin–Reduskevich isotherm plots for the removal of procion orange by coir pith carbon.

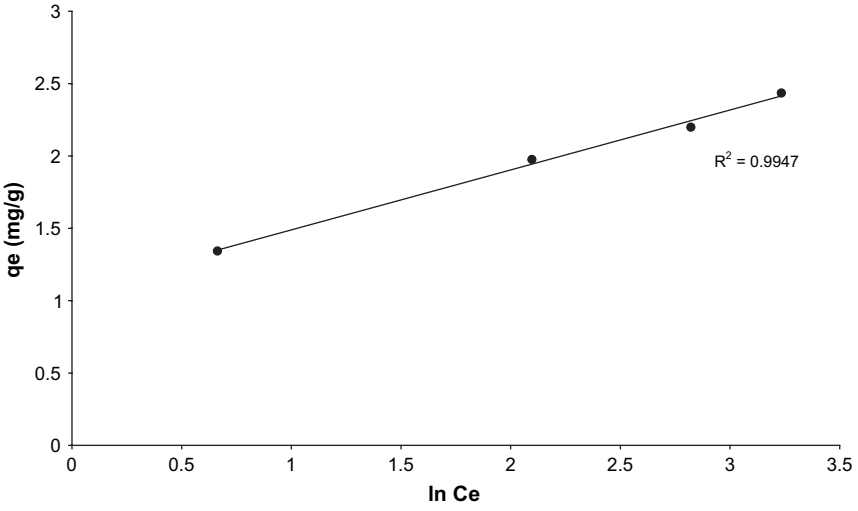

Fig. 10. Tempkin isotherm plots for the removal of procion orange by coir pith carbon.

3.7.4. Tempkin isotherm

The derivation of the Temkin isotherm assumes that the fall in the heat of sorption is linear rather than logarithmic, as implied in the Freundlich equation [43]. The Temkin isotherm has generally been applied in the following form [44]:

$$q_e = \mathrm{RT}/b \ln (K_t C_e) \quad (12)$$

Eq. (11) can be expressed in its linear form as:

$$q_e = B_1 \ln K_t + B_1 \ln C_e \quad (13)$$

where

$$B_1 = \mathrm{RT}/b \quad (14)$$

The adsorption data can be analyzed according to Eq. (12). A plot of q_e versus ln C_e enables the determination of the isotherm constants K_t and B_1. K_t is the equilibrium binding constant (l/min) corresponding to the maximum binding energy and constant B_1 is related to the heat of adsorption. This isotherm for the adsorption of procion orange on coir pith carbon is depicted in Fig. 10 and values of the parameters are given in Table 3.

3.8. Pore diffusion coefficient

Assuming spherical geometry for the adsorbent, the time for half adsorption can be correlated to the pore diffusion coefficient [45]

$$t_{1/2} = 0.03 r_0^2 / D_p \quad (15)$$

where $t_{1/2}$ is the time for half adsorption (s), r_0 is the radius of the adsorbent particle (cm) and D_p is the diffusion coefficient (cm^2/s). Values of D_p have been calculated for different temperatures and different concentrations of dye. The removal of dye follows pore diffusion process since the coefficient

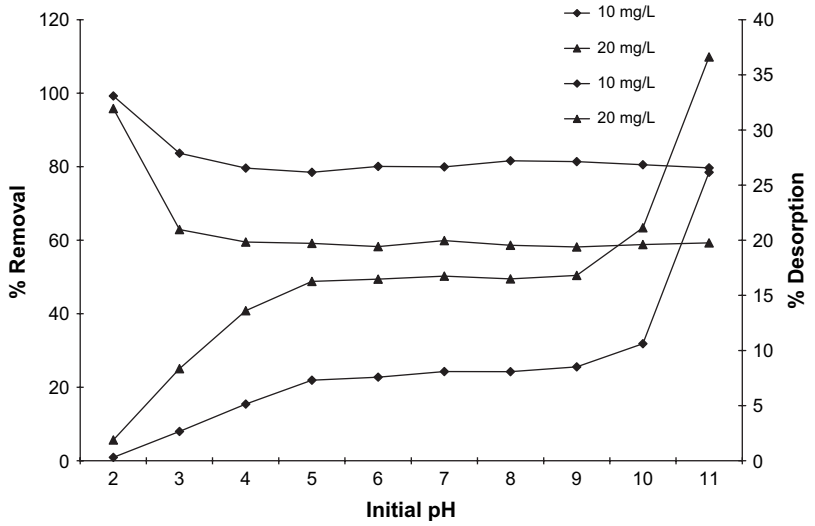

Fig. 11. Effect of pH on removal of procion orange: adsorbent dose, 300 mg/50 ml; 10 mg/L, agitation time 40 min; 20 mg/L, agitation time 60 min. (B) Effect of pH on desorption of dye from dye-loaded adsorbent: adsorbent dose, 300 mg/50 ml; 10 mg/L, agitation time 40 min; 20 mg/L, agitation time 60 min.

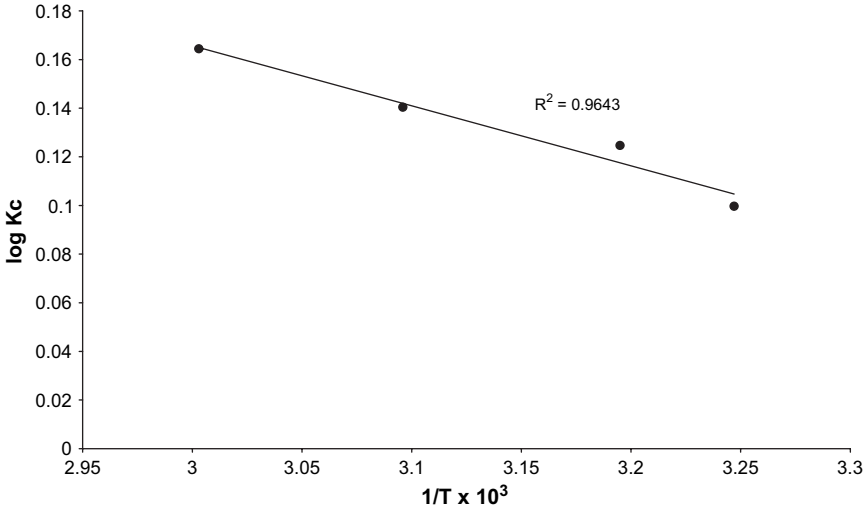

Fig. 12. van't Hoff plot for the adsorption of procion orange.

values are in the range of 10^{-11}–10^{-13} cm^2/s. Values of D_p for procion orange are 1.178 cm^2/s for 10–40 mg/L and 0.393 cm^2/s for 10 mg/L of dye in the temperature range 35–60 °C.

3.9. Studies on pH effect

The influence of pH on the adsorption capacity of coir pith carbon for the removal of procion orange is studied (Fig. 11). Activated carbon normally contains varying amounts of water molecules especially those which either exist as surface hydroxyl groups or adsorbed water. At acidic pH, an increasing concentration of the H^+ ion in dye solution, the surface OH^- ions would get neutralized by protonation, which facilitates the diffusion of dye molecules in the vicinity of the adsorbent. Consequently the positive charge density would be located more on the dye molecule at pH 2, and this accounts for the higher dye uptake on the negatively charged surface. Thus it seems likely that the negative charge density on the surface will increase and will be associated with H^+ or Na^+ ions according to the pH of the solution. These positively charged ions in the presence of dye solution could then be exchanged with dye cations as follows:

$$MO^- \left| \begin{matrix} H^+ \\ \\ Na^+ \end{matrix} \right. \quad Dye^+\text{-----}Cl^- \quad MO^- \left| \; Dye^+ \right.$$

At solution pH = 2.0, the surface becomes positively charged and is associated with negatively charged Cl^-:

$$MOH_2^+ \left| \; Cl^- \right.$$

Obviously, there will be no exchangeable cationic species on the adsorbent surface in alkaline medium, resulting in unfavorable conditions for the adsorption of the dye. It shows that the adsorption was decreased as the pH of the system increases, when the number of negative charge on the surface is very much reduced due to the excess of protons in solution. A negatively charged surface site on the adsorbent does not favor the adsorption of dye anions due to the electrostatic repulsion. This suggests that chemisorption plays a main role in the adsorption.

3.10. Desorption studies

Desorption studies help to elucidate the mechanism of adsorption and also help in the recovery of dye and adsorbent, which makes the treatment process more economical, and it is necessary to regenerate the spent carbon and dye. As the desorbing pH was increased, the percent removal increased from 0.31 at pH 2 to 26.16 at pH 11 for 10 mg/L and 1.89 at pH 2 to 36.62 at pH 11 for 20 mg/L (Fig. 11). A maximum desorption occurred at alkaline pH.

3.11. Effect of temperature

Increase of temperature increased the percent removal. Changes in standard free energy, enthalpy and entropy of adsorption were calculated using the following equations:

$$\Delta G^\circ = -RT \ln K_c \tag{16}$$

where R is gas constant, K_c is the equilibrium constant and T is the temperature in K.

According to van't Hoff equation

Table 4
Thermodynamic parameters

Temp (°C)	Kc	ΔG° (kJ/mol)	ΔH° (kJ/mol)	ΔS° (J/k/mol)
35	1.258	−0.588	4.726	17.35
40	1.333	−0.736		
50	1.382	−0.828		
60	1.46	−0.969		

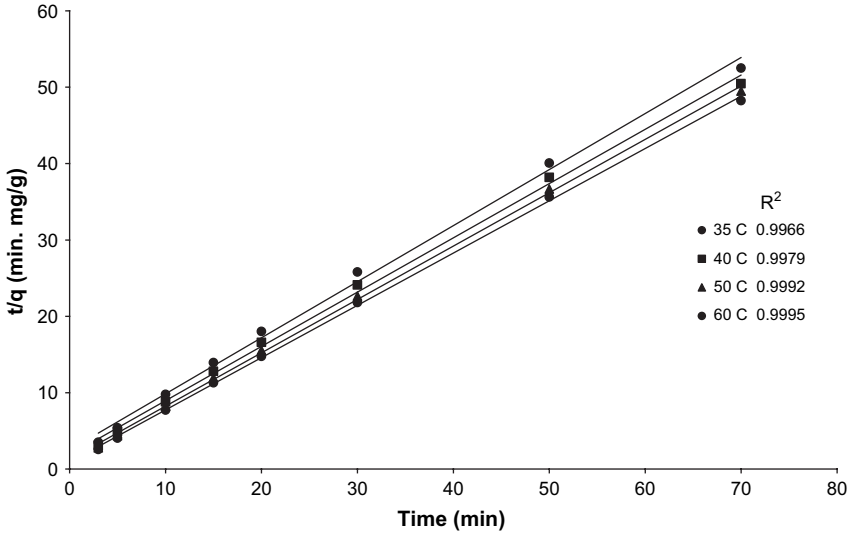

Fig. 13. Second-order kinetic at different temperatures: adsorbent dose, 200 mg/50 ml; procion orange concentration, 10 mg/L; initial pH, 6.9.

$$\log_{10}K_c = \Delta S^{\circ}/2.303R - \Delta H^{\circ}/2.303\mathrm{RT} \quad (17)$$

Plot of log K_c versus $1/T$ is linear (Fig. 12). Values of ΔH° and ΔS° were evaluated from the slope and intercept of van't Hoff plot, respectively (Table 4). Positive values of ΔH° show the endothermic nature of adsorption. The negative values of ΔG° indicate the spontaneous nature of adsorption for procion orange at 35, 40, 50 and 60 °C. Entropy of activation can be regarded as a measure of the "saddle point of energy" over which reactant molecules must pass as activated complexes. Thus ΔS° conveys whether a particular reaction proceeds faster or slower than another individual reaction [40]. The positive values of ΔS° suggest the increased randomness at the solid/solution interface during the adsorption of dye on coir pith carbon. Linear plots of t/q versus t corresponding to the second-order kinetic model were obtained (Fig. 13). Intra-particle diffusion plot for q_t versus $t^{1/2}$ should be a straight line (Fig. 14) and double logarithmic plot of loglog $(C_0/C_0 - q_t m)$ versus log t (Fig. 15) also yielded perfect linear curves for procion orange at different temperature studies. The equilibrium data obtained for all the kinetics are presented in Table 2.

4. Conclusions

The present study shows that coir pith carbon is an effective adsorbent for the removal of procion orange from aqueous solution. The Physico-chemical characteristics of having an excess of positive charge on the surface enabled activated carbon to adsorb procion orange with a greated capacity. With respect to the suitability of the first-order and second-order kinetic models for procion orange adsorption onto carbon, it has been represented that the adsorption kinetics of procion

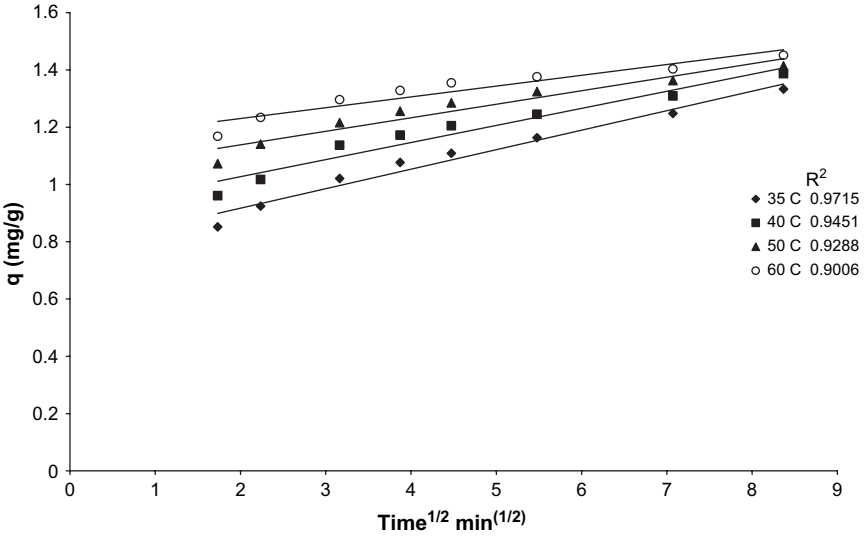

Fig. 14. Weber and Morris intra-particle diffusion plots for removal of procion orange at different temperatures: adsorbent dose, 200 mg/50 ml; procion orange concentration, 10 mg/L; initial pH, 6.9.

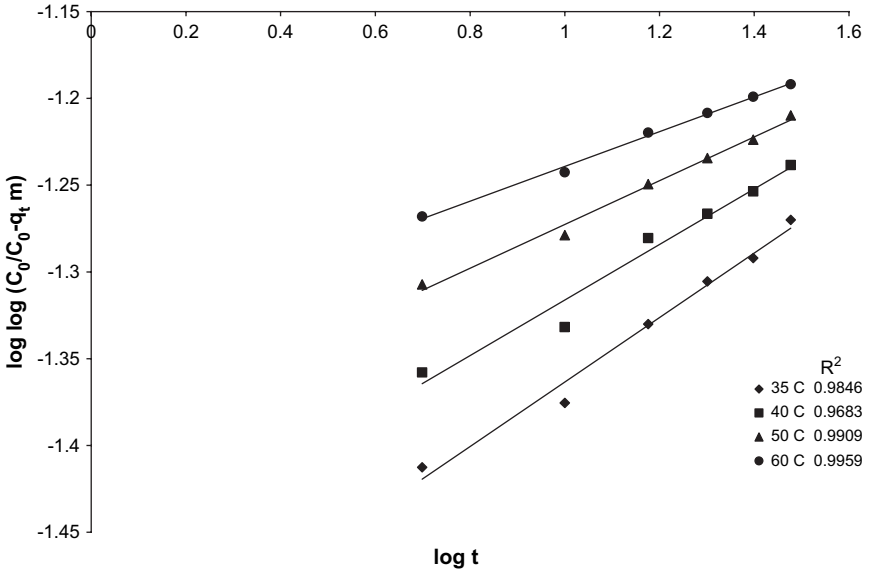

Fig. 15. Bangham plot for removal of procion orange at different temperatures: adsorbent dose, 200 mg/50 ml; procion orange concentration, 10 mg/L; initial pH, 6.9.

orange obeys the second-order kinetics preferably, which provide the best correlation of the data. However, there is evidence that the adsorption of dye onto coir pith carbon is a complex process, so it cannot be adequately described by a single kinetic model throughout the whole process. In this manner, for instance, intra-particle diffusion played a significant role, but it was not the main rate determining step during adsorption. By comparing the correlation coefficients determined for each linear transformation of isotherm analysis, the Langmuir and Tempkin isotherm models, which fit the experimental data reasonably well, were found to provide the best prediction for the adsorption of procion orange. The activation energy of adsorption can be evaluated with the second-order rate constants. Since the raw material coir pith is freely available in large quantities in coir industries, the treatment method seems to be economical. Based on the above good results this relatively cheap, low-cost material is recommended as an effective and cheap adsorbent for removal of dye from textile effluents.

References

[1] Forgacs E, Cserhati T, Oros G. Removal of synthetic dyes from wastewaters: a review. Environment International 2004;30:953.
[2] Robinson T, McMullan G, Marchant R, Nigam P. Remediation of dyes in textile effluent: a critical review on current treatment technologies with a proposed alternative. Bioresource Technology 2001;77:247.
[3] Papic S, Koprivanac N, Bozic AL, Metes A. Removal of some reactive dyes from synthetic wastewater by combined Al(III) coagulation/carbon adsorption process. Dyes Pigments 2004;62:291.
[4] Raymound EK, Dunald F. Encyclopedia of chemical technology. New York: Wiley; 1984.
[5] Lee JW, Choi SP, Ramesh T, Shim WG, Moon H. Evaluation of the performance of adsorption and coagulation processes for the maximum removal of reactive dyes. Dyes and Pigments 2006;69:196.
[6] Chern JM, Huang SN. Study of nonlinear wave propagation theory: 1. Dye adsorption by activated carbon. Industrial Engineering and Chemistry Research 1998;37:253.
[7] Ozacar M, Sengil IA. Adsorption of reactive dyes on calcined alunite from aqueous solutions. Journal of Hazardous Material 2003;B98:211.
[8] Selva roselin GR, Rajarajeswari R, Selvin V, Sadasivam B, Sivasankar, Rengaraj K. Sunlight/Zno-mediated photocatalytic degradation of reactive red 22 using thin film bed flow photoreacter. Solar Energy 2002;73:281.
[9] Kabdasli I, Olmez T, Tunay O. Factors affecting colour removal from reactive dye bath by ozonation. Water Science and Techology 2002;45:261.
[10] Hassan MM, Hawkyard CJ. Ozonation of aqueous dyes and dye house effluent in a bubble-column reactor. Journal of Environmental Science and Health. Part A- Toxic/Hazardous Substance and Environmental Engineering 2002;A37:1563.
[11] Liu HJ, Qu JH. Decolorization of reactive bright red K2G dye: electrochemical process catalyzed by manganese mineral. Water Science and Technology 2002;46:133.
[12] Stephenson RJ, Stephenson JB. Coagulation and precipitation of a mechanism pulping effluent. Water Research 1996;30:7781.
[13] Churchley JH. Removal of dye wastewater color from sewage effluent—the use of full scale ozone plant. Water Science and Technology 1994;30:275.
[14] Laszlo JA. Removing acid dyes from textile wastewater using biomass for decolourization. American Dyes Stuff Report 1994;83:17.
[15] Ince NH, Hasan DA, Ustun B, Tezcanli G. Combinative dye bath treatment with activated carbon UV/H_2O_2: a case study on Everzol Black-GSP. Water Science and Technology 2002;46:51.
[16] Kornmuller A, Karcher, Jekel M. Adsorption of reactive dyes to granulated iron hydroxide and its oxidative regeneration. Water Science and Technology 2002;46:43.
[17] Asfour HM, Fadali OA, Nassar MM, El-Geundi MS. Equilibrium studies on adsorption of basic dyes on hard wood. Journal of Chemical Technology and Biotechnology 1995;35A:293.
[18] Desai M, Dogra A, Vora S, Bahadur P, Ram RN. Adsorption of some acid dyes from aqueous solution onto neutral alumina. Indian Journal of Chemistry 1997;36A:938.
[19] Meshko V, Markovska MN, Schucmann HP, Sonntag C. A chemical actinometer for use in connection with UV treatment in drinking water processing. Journal of Water SRT- Aquo 1990;39:309.
[20] Guo Y, Zhao J, Zhang H, Yang S, Qi J, Wang Z, et al. Use of rice husk-based porous carbon for adsorption of Rhodamine B from aqueous solutions. Dyes and Pigments 2005;66:123.
[21] Robinson T, Chandran B, Sathya Naidu G, Nigam P. Studies on the removal of dyes from a synthetic textile effluent using barley husk in static-batch mode and in a continuous flow, packed-bed, reactor. Bioresource Technology 2002;85:43.

[22] Mittala A, Krishnanav L, Guptab VK. Removal and recovery of malachite green from wastewater using an agricultural waste material, de-oiled soya. Separation and Purification Technology 2005;43:125.
[23] Silva JP, Sousa S, Rodrigues J, Antunes H, Porter JJ, Gonçalves I, et al. Adsorption of acid orange 7 dye in aqueous solutions by spent brewery grains. Separation and Purification Technology 2004;40:309.
[24] Mall ID, Srivastava VC, Agarwal NK. Removal of Orange-G and Methyl Violet dyes by adsorption onto bagasse fly ash-kinetic study and equilibrium isotherm analyses. Dyes and Pigments 2006;69:210.
[25] Ilhan Uzun. Kinetics of the adsorption of reactive dyes by chitosan. Dyes and Pigments 2006;70:76.
[26] Gonga R, Suna Y, Chenb J, Liua H, Yang C. Effect of chemical modification on dye adsorption capacity of peanut hull. Dyes and Pigments 2005;67:175.
[27] Bhattacharyya KG, Sharma A. Kinetics and thermodynamics of Methylene Blue adsorption on neem (*Azadirachta indica*) leaf powder. Dyes and Pigments 2005;65:51.
[28] McKay G, Bino MJ, Altamemi AR. The adsorption of various pollutants from aqueous solutions onto activated carbon. Water Research 1985;19:491.
[29] Nelly JW, Isacoff EG. Carbonaceous adsorbents for the treatment of ground and surface water. New York: Marcel Dekker; 1982.
[30] Rook JJ. Treatment of water by granular activated carbon. In: McGuire MJ, Suffet IH, editors. Washington, DC: American Chemical Society; 1983.
[31] Lagergren S, Svenska BK. 1898 Zur theorie der sogenannten adsorption geloester stoffe. Vetenskapsakad. Handl 1982;24:1.
[32] McKay G, Ho YS. Pseudo-second order model for sorption processes. Process Biochemistry 1999;34:451.
[33] Weber Jr WJ, Morris JC. Kinetics of adsorption on carbon from solution. Journal of the Sanitary Engineering Division, American Society of Civil Engineers 1963;89:31.
[34] Kannan K, Sundaram MM. Kinetics and mechanism of removal of methylene blue by adsorption on various carbons—a comparative study. Dyes and Pigments 2001;51:25.
[35] Aharoni C, Sideman S, Hoffer E. Adsorption of phosphate ions by colloid ion-coated alumina. Journal of Chemical Technology and Biotechnology 1979;29:404.
[36] Tutem E, Apak R, Unal CF. Adsorptive removal of chlorophenols from water by bituminous shale. Water Research 1998;32:2315.
[37] Langmuir I. The adsorption of gases on plane surfaces of glass, mica and platinum. Journal of the American Chemical Society 1918;40:1361.
[38] Namasivayam C, Muniasamy N, Gayatri K, Rani M, Ranganathan K. Removal of dyes from aqueous solutions by cellulosic waste orange peel. Bioresource Technology 1996;57:37.
[39] Weber TW, Chakkravorti P. Pore and solid diffusion models for fixed-bed adsorbers. AIChEJ 1974;20:228.
[40] Freundlich H. Uber die Adsorption in lunsungen. Journal of Physical Chemistry 1985;57:387.
[41] Dubinin MM. The potential theory of adsorption of gases and vapors for adsorbents with energetically non-uniform surface. Chemical Reviews 1960;60:235.
[42] Hasany SM, Chaudhary MH. Sorption potential of Hare river sand for the removal of antimony from acidic aqueous solution. Applied Radiation and Isotopes 1996;47:467.
[43] Aharoni C, Sparks DL. Kinetics of soil chemical reactions – a theoretical treatment. In: Sparks DL, Suarez DL, editors. Rates of soil chemical processes. Madison, WI: Soil Science Society of America; 1991. p. 1–18.
[44] Aharoni C, Ungarish M. Kinetics of activated chemisorption. Part 2. Theoretical models. Journal of the Chemical Society Faraday Transactions 1977;73:456.
[45] Michelson LD, Gideon PG, Pace EG, Kutal LH. Removal of soluble mercury from wastewater by complexing technique. US Department of Industry, Office of Water Research and Technology; 1975. Bull. No. 74.